C/EBPα regulates osteoclast lineage commitment

Wei Chen[1], Guochun Zhu, Liang Hao, Mengrui Wu, Hongliang Ci, and Yi-Ping Li[1]

Department of Pathology, University of Alabama at Birmingham, Birmingham, AL 35294-2182

Edited by Gerard Karsenty, Columbia University, New York, NY, and accepted by the Editorial Board February 7, 2013 (received for review July 5, 2012)

Despite recent insights gained from the effects of targeted deletion of the *Finkel-Biskis-Jinkins osteosarcoma oncogene (c-fos)*, *Spleen focus-forming virus* (*SFFV*) *proviral integration 1 (PU.1)*, *microphthalmia-associated transcription factor*, *NF-κB*, and *nuclear factor of activated cells cytoplasmic 1* (*NFATc1*) transcription factor genes, the mechanism underlying transcription factors specifying osteoclast (OC) lineage commitment from monocyte/macrophage remains unclear. To characterize the mechanism by which transcription factors regulate OC lineage commitment, we mapped the critical *cis*-regulatory element in the promoter of *cathepsin K* (*Ctsk*), which is expressed specifically in OCs, and found that CCAAT/enhancer binding protein α (C/EBPα) is the critical *cis*-regulatory element binding protein. Our results indicate that C/EBPα is highly expressed in pre- OCs and OCs. The combined presence of macrophage colony-stimulating factor and receptor activator of NF-κB ligand significantly induces high C/EBPα expression. Furthermore, *C/EBPα*$^{-/-}$ newborn mice exhibited impaired osteoclastogenesis, and a severe osteopetrotic phenotype, but unaffected monocyte/macrophage development. Impaired osteoclastogenesis of *C/EBPα*$^{-/-}$ mouse bone marrow cells can be rescued by *c-fos* overexpression. Ectopic expression of C/EBPα in mouse bone marrow cells and monocyte/macrophage cells, in the absence of receptor activator of NF-κB ligand, induces expression of *receptor activator of NF-κB*, *c-fos*, *Nfatc1*, and *Ctsk*, and it reprograms monocyte/macrophage cells to OC-like cells. Our results demonstrate that C/EBPα directly up-regulates *c-fos* expression. C/EBPα$^{+/-}$ mice exhibit an increase in bone density compared with C/EBPα$^{+/+}$ controls. These discoveries establish C/EBPα as the key transcriptional regulator of OC lineage commitment, providing a unique therapeutic target for diseases of excessive bone resorption, such as osteoporosis and arthritis.

cell lineage commitment | gene expression regulation | osteoclast differentiation | bone homeostasis | osteopetrosis phenotype

Osteoclasts (OCs), bone-resorbing cells, play a key role in normal bone remodeling and in many diseases, such as osteopetrosis, osteoporosis, arthritis, periodontal disease, and certain bone metastases. OCs develop from monocytic precursors from the hematopoietic lineage. *Spleen focus-forming virus* (*SFFV*) proviral integration 1 (PU.1) can induce the expression of the macrophage colony-stimulating factor (M-CSF) receptor and is critical for monocyte/macrophage lineage commitment (1). On receptor activator of NF-κB ligand (RANKL) stimulation and immunoreceptor tyrosine-based activation motif (ITAM) activation, OC precursors undergo further differentiation to mononuclear OCs (2). RANKL specifically and potently induces nuclear factor of activated T cells cytoplasmic 1 (NFATc1), which is a master regulator of OC differentiation, through both the TNF receptor-associated factor 6 (TRAF6)–NF-κB (p105n) pathway and the *Finkel-Biskis-Jinkins osteosarcoma oncogene* (*c-Fos*) pathway (3–7). This robust induction of NFATc1 is based on an autoamplifying mechanism effected through persistent calcium signal-mediated activation of NFATc1 (NFATc1 binds to NFAT binding sites on its own promoter, constituting a positive feedback loop) (7). In the nucleus, NFATc1 cooperates with other transcription factors, such as activator protein-1, PU.1, cAMP-responsive element binding protein, and microphthalmia-associated transcription factor, to induce various OC-specific genes (7, 8). NFATc1, together with other transcription factors, such as *c-fos* and NF-κB, drives osteoclastogenesis (2, 5). Peroxisome proliferator-activated receptor γ (PPARγ) is also reported to be important for OC differentiation (9). Although much has been revealed pertaining to the regulation of terminal differentiation of OCs, the cascade of transcription factors that specifies OC lineage commitment from monocytes/macrophages remains unclear (10). Indeed, a long-standing challenge remaining in the field is to define the mechanism by which M-CSF acts with RANKL to promote OC differentiation, whereas it promotes macrophage differentiation when acting alone (10), and to define the factor that regulates OC lineage commitment.

Cathepsin K (*Ctsk*) is a lysosomal cysteine protease that is abundantly and selectively expressed in OCs (11).The specific expression of the *Ctsk* in OCs, as well as its enzymatic properties, implies that it has a key role in normal bone remodeling and in pathological processes, such as osteoporosis, osteoarthritis, and pycnodysostosis (12). Because expression of *Ctsk* is OC-specific and induced by RANKL stimulation, we characterized the *Ctsk* critical *cis*-regulatory elements (CCREs) to identify the transcription factor(s) that modulate OC-specific gene (e.g., *Ctsk*) expression and to determine which factor(s) enable monocytes to commit to the OC lineage after RANKL stimulation.

Our research revealed that CCAAT/enhancer binding protein α (C/EBPα) regulates OC cell lineage commitment and differentiation. C/EBPα is a key molecular determinant in myeloid lineage commitment (13, 14), which drives myeloid differentiation through activation of myeloid target genes and through inhibition of the cell cycle through interactions with regulatory proteins (15, 16). We characterized C/EBPα as the binding protein of the OC gene *Ctsk* CCRE. We found that the deletion of *C/EBPα* in KO mice results in severely blocked osteoclastogenesis and that the overexpression of *c-fos* rescues osteoclastogenesis when *C/EBPα* is knocked out. Forced expression of *C/EBPα*, in the absence of RANKL, induces expression of *receptor activator of NF-κB* (*RANK*) and OC genes and reprograms the monocyte/macrophage cell line to OC-like cells. These discoveries establish C/EBPα as the key regulator of OC lineage commitment.

Results

Identification of Mouse *Ctsk* CCRE and Characterization of CCRE DNA Binding Protein. To understand the transcription factors that modulate OC gene expression and OC differentiation, we characterized the *Ctsk* CCREs. Our results show that RANKL stimulates *Ctsk* gene promoter activity and indicate the importance of RANKL in combination with the CCRE (Fig. 1*A*). To analyze the −137 to −31 region identified as containing a potential CCRE further, we examined the effect of internal deletions within the promoter-CAT fusion gene (pCCAT)-137 construct on *Ctsk* activity and found that internal deletions of the sequence between −51 and −34 or between −46 and −41 resulted in the total loss of *Ctsk* promoter activity compared with the complete

Author contributions: W.C. and Y.-P.L. designed research; W.C., G.Z., L.H., M.W., H.C., and Y.-P.L. performed research; W.C., G.Z., L.H., M.W., H.C., and Y.-P.L. analyzed data; and W.C. and Y.-P.L. wrote the paper.

The authors declare no conflict of interest.

This article is a PNAS Direct Submission. G.K. is a guest editor invited by the Editorial Board.

[1]To whom correspondence should be addressed. E-mail: ypli@uab.edu or wechen@uab.edu.

This article contains supporting information online at www.pnas.org/lookup/suppl/doi:10.1073/pnas.1211383110/-/DCSupplemental.

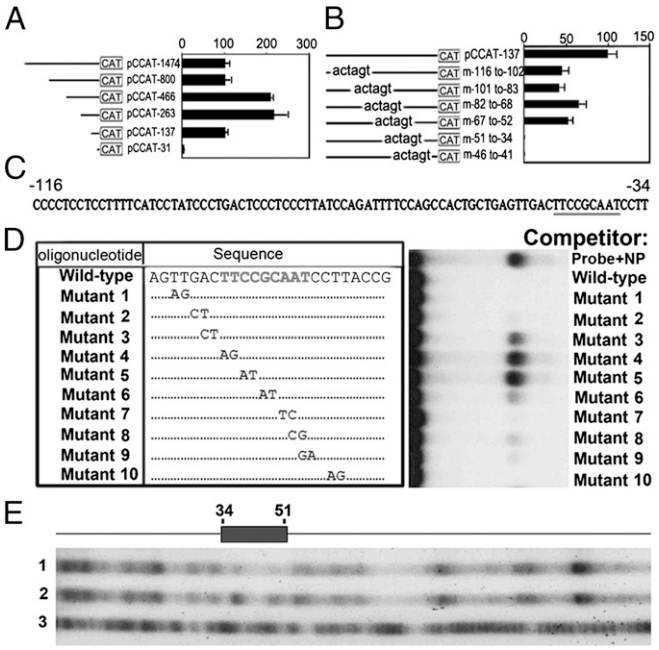

Fig. 1. Identification of *Ctsk* CCRE and CCRE DNA binding protein as C/EBPα. (*A*) Activity of deletion mutants of the pCCAT construct was measured in RANKL-induced RAW64.7 cells. Schematic representation of each reporter construct is shown. Values are relative to the activity obtained with the largest promoter fragment (pCCAT-1474). CAT activities are normalized with the cotransfected β-gal activity. Experimental data are reported as mean ± SD of triplicate independent samples ($n = 5$, repeated three times). (*B* and *C*) Summary of site-specific mutagenesis of the *Ctsk* promoter binding site from −116 to −34 and characterization of the CCRE as a C/EBPα site. (*D*) Gel mobility shift experiment using a ^{32}P-labeled −53 to −30 WT *Ctsk* promoter oligonucleotide probe in nuclear extracts prepared from RANKL-induced RAW264.7 cells, with and without 100-fold molar excess of unlabeled WT or mutant oligonucleotides as described on the left. NP, nuclear protein. (*E*) DNase I footprint assays identify a binding site between −34 to −51 in the −137 to −31 mouse *Ctsk* promoter. The protected region is indicated by a shaded box, which contains a C/EBPα site. DNase I digestion of the naked DNA incubated with (lane 1) and without (lane 2) RANKL-induced RAW264.7 cell nuclear extracts is shown. G + A Maxam–Gilbert reaction of the −137 to −31 promoter fragment is shown in lane 3.

pCCAT-137 construct (Fig. 1*B*). Thus, we determined that the sequence between −51 and −34 contains a *Ctsk* CCRE (Fig. 1*C*). We performed a gel mobility shift experiment using the ^{32}P-labeled WT *Ctsk* oligonucleotide probe in nuclear extracts prepared from mouse OC precursor cell line RAW264.7 cells induced with RANKL, with and without a 100-fold molar excess of unlabeled WT or 10 different mutant oligonucleotides. We found that a 100-fold molar excess of mutants 3 and 6 partially competes, whereas mutants 4 and 5 are completely unable to compete, for the DNA–protein complex, indicating that this core sequence of nucleotides is essential for DNA–protein interaction (Fig. 1*D*). We analyzed this sequence using transcription factor binding site database searches and found that it is a C/EBPα binding site (TTCCGCAAT). This indicates that C/EBPα may regulate the CCRE. We also performed DNase I footprint analysis and found that the −51 to −34 region, which contains the C/EBPα binding site, was protected (Fig. 1*E*). To confirm that C/EBPα binds to this CCRE recognition site, we performed supershift mobility assays using a panel of specific antibodies against different C/EBP family members (Fig. S1). The bound proteins only produced supershifted complexes in the presence of C/EBPα antibody, indicating that C/EBPα is involved in the formation of this DNA–protein complex (Fig. S1). Together, these data indicate that *C/EBPα* may be a major component of the OC-specific complex that regulates the *Ctsk* CCRE.

C/EBPα Is Expressed in Pre-OCs and OCs and Is Induced by RANKL. We next examined the tissue and cellular distribution of *C/EBPα* mRNA by performing a Northern hybridization assay. Giant cell tumors (GCTs) of bone contain human stromal cells (hSCs), OC-like precursors, and OC-like giant cells. Because OC-like giant cells from GCTs of bone are effectively the same as OCs in bone, we used GCTs and hSCs obtained as previously described (11). In addition, RANKL-induced mouse bone marrow (MBM), uninduced MBM, rat osteoblast, and a human macrophage cell line (U-937 cells) were used along with *C/EBPα*$^{+/+}$ mouse tissues. The human C/*EBPα* transcript (2.4 kb) and mouse C/*EBPα* transcript (2.7 kb) used as C/*EBPα*-cDNA probes for this Northern blot assay are highly specific to C/*EBPα*. As shown in Fig. 2*A*, C/EBPα (2.7 kb) was highly expressed in RANKL-induced MBM and *C/EBPα*$^{+/+}$ liver tissue. *C/EBPα* (2.4 kb) was prominently expressed in GCTs of bone (which contain hSCs, OC-like precursors, and OC-like giant cells) but was not expressed in hSCs (Fig. 2*A*). Furthermore, there was very low C/*EBPα* expression in U-937 cells, MBM, and mouse kidney and brain tissue. Expression of C/*EBPα* could not be detected in other tissues in these conditions, but this

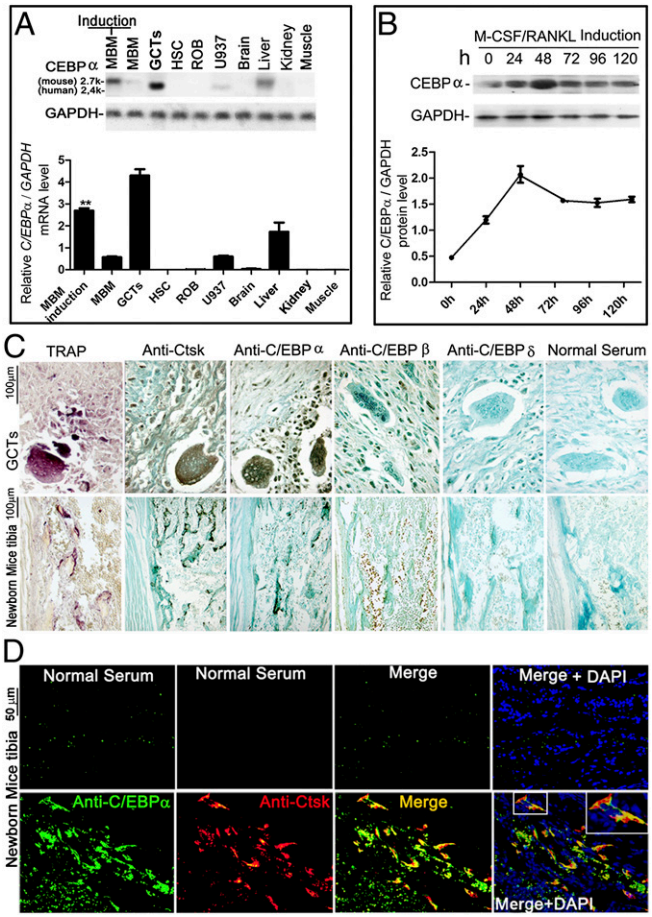

Fig. 2. C/EBPα is expressed in pre-OCs and OCs, and it is induced by RANKL. (*A*) Northern blot hybridization using a *C/EBPα*-specific probe in RANKL-induced and uninduced *C/EBPα*$^{+/+}$ MBM, GCTs of bone, hSCs, rat osteoblast (ROB), a human macrophage cell line (U-937 cells), and *C/EBPα*$^{+/+}$ mouse tissues. (*B*) Time-course Western blot analysis of C/EBPα expression in *C/EBPα*$^{+/+}$ MBM cultured with M-CSF (20 ng/mL) alone for 2 d and then stimulated with M-CSF (10 ng/mL)/RANKL (10 ng/mL) for 0–120 h. (*C*) TRAP staining and immunostaining for Ctsk, C/EBPα, C/EBPβ, and C/EBPδ in GCTs of bone and *C/EBPα*$^{+/+}$ tibiae sections. Normal serum is shown as a control. (*D*) Immunofluorescence staining of C/EBPα (green) and Ctsk (red) in *C/EBPα*$^{+/+}$ tibiae indicates significant overlap, visualized as a yellow area in the merged image ($n > 9$). *Inset* is the magnified image of the boxed area.

does not exclude a role for C/*EBPα* in those tissues. In order to characterize C/EBPα expression during OC differentiation, we performed Western blot analysis of C/EBPα expression in MBM cultured with M-CSF (20 ng/mL) alone for 2 d and then stimulated with M-CSF (10 ng/mL)/RANKL (10 ng/mL) for 0–120 h. We found that C/EBPα expression more than doubled after 24 h of stimulation. Interestingly, C/EBPα expression peaked at 48 h but retained high expression thereafter (Fig. 2*B*). The dramatic increase in C/EBPα expression early during OC differentiation indicates that C/EBPα may play a critical role in the regulation of OC commitment and OC differentiation. To determine the expression of Ctsk and C/EBP family members (i.e., C/EBPα, C/EBPβ, C/EBPδ) in situ, OC cells were subjected to immunohistochemical staining (17). We found strong C/EBPα expression in Ctsk-positive multinucleated OCs and mononuclear pre-OCs in GCTs and *C/EBPα*$^{+/+}$ tibiae in a similar pattern of expression as Ctsk (Fig. 2*C*). In contrast, C/EBPβ was weakly expressed in TNF receptor-associated protein 1 (TRAP)-positive mononuclear pre-OCs, and C/EBPδ expression was not detected in GCTs or *C/EBPα*$^{+/+}$ tibiae (Fig. 2*C*). Immunofluorescence staining of *C/EBPα*$^{+/+}$ tibiae also revealed that C/EBPα colocalized with Ctsk (Fig. 2*D*). The pattern of C/EBPα expression indicates a possible critical function of C/EBPα in OC cell lineage commitment and differentiation.

***CEBPα*$^{-/-}$ Newborn Mice Exhibited a Severe Osteopetrotic Phenotype Due to Impaired Osteoclastogenesis.** X-ray analyses revealed that *C/EBPα*$^{-/-}$ mice have dramatically increased bone density compared with *C/EBPα*$^{+/+}$ mice (Fig. 3*A*), indicating that *C/EBPα*$^{-/-}$ mice have an osteopetrotic phenotype. This is supported by microcomputed tomography analysis, which showed significantly increased bone volume and bone mineral density in *C/EBPα*$^{-/-}$ femora compared with *C/EBPα*$^{+/+}$ femora (Fig. 3 *B* and *C*). In order to analyze the role of C/EBPα in OCs further, we examined whether a null mutation in *C/EBPα* alleles affects the differentiation of OCs (17). Our histochemical stains revealed that *C/EBPα*$^{-/-}$ mice tibiae have long growth plates and a dramatic reduction in TRAP^{+} OCs compared with *C/EBPα*$^{+/+}$ controls (Fig. 3*D*). Furthermore, TRAP stains demonstrated that TRAP^{+} multinucleated OCs were not formed in RANKL-induced MBM culture from *C/EBPα*$^{-/-}$ mice compared with *C/EBPα*$^{+/+}$ controls (Fig. 3*E*). These data confirm that *C/EBPα*$^{-/-}$ mice are osteopetrotic and indicate that this phenotype is mainly due to defective osteoclastogenesis. In order to determine if *C/EBPα*$^{-/-}$ osteoblasts contribute to the defective osteoclastogenesis observed in *C/EBPα*$^{-/-}$ mice, we used a coculture system and TRAP stain as we have previously described (17). We determined that a coculture of calvarial mouse osteoblasts (MOBs) derived from *C/EBPα*$^{+/+}$ mice with MBM from *C/EBPα*$^{-/-}$ mice is unable to rescue osteoclastogenesis (compared with *C/EBPα*$^{+/+}$ MOBs with *C/EBPα*$^{+/+}$ MBM) (Fig. 3*F*). Coculture of *C/EBPα*$^{-/-}$ MOBs with *C/EBPα*$^{+/+}$ MBM revealed that mutant osteoblasts sustain osteoclastogenesis (Fig. 3*F*), indicating that osteoblasts lacking *C/EBPα* do not contribute to the defective osteoclastogenesis in *C/EBPα*$^{-/-}$ mice.

***C/EBPα* KO Reduces the Expression of OC Differentiation Regulator and Marker Genes.** To determine the mechanism of *C/EBPα* function in OC commitment and differentiation, we performed real-time (RT) quantitative PCR (qPCR) analysis of gene expression in *C/EBPα*$^{+/+}$ and *C/EBPα*$^{-/-}$ MBM cells cultured with M-CSF/RANKL to generate OC-like cells (Table S1) (12, 17, 18). The RT-qPCR results (Fig. S2) suggest that *C/EBPα* is important for the induction of OC-specific genes and that *C/EBPα* may suppress macrophage-specific genes. These results were confirmed by Western blot analysis of C/*EBPα*$^{+/+}$ and *C/EBPα*$^{-/-}$ MBM cells-derived OC-like cells, which showed that Ctsk, *c-fos*, and Nfatc1 decreased in *C/EBPα*$^{-/-}$ cells compared with control (Fig. 4*A*). Additionally, there was a significant difference in the protein level of PU.1 in C/*EBPα*$^{+/+}$ and *C/EBPα*$^{-/-}$ MBM cells OC-like cells (Fig. 4 *A* and *B*). Time-course

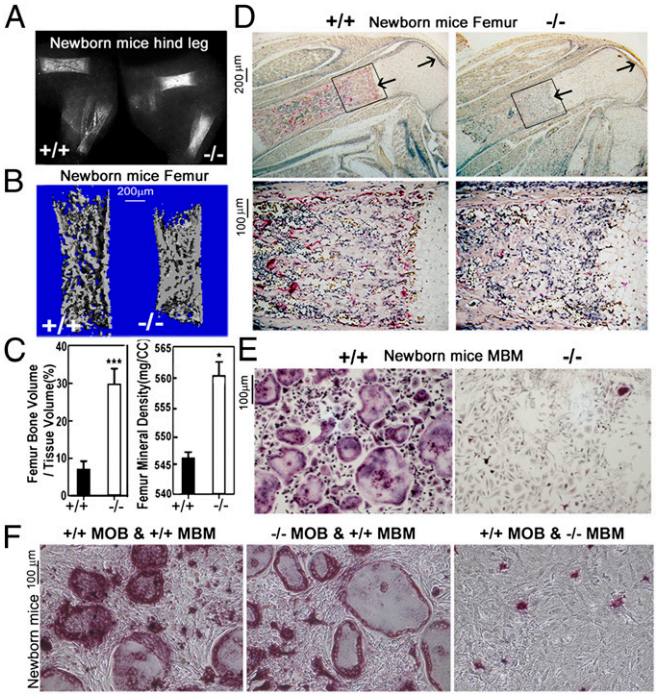

Fig. 3. Increased bone mass and defective osteoclastogenesis in *C/EBPα*$^{-/-}$ mice in vivo and in vitro. (*A*) Radiographic analysis of femora and tibiae indicates osteopetrosis in *C/EBPα*$^{-/-}$ newborn mice compared with *C/EBPα*$^{+/+}$ newborn mice (n = 5, repeated three times). (*B*) Three-dimensional microcomputed tomography images of *C/EBPα*$^{+/+}$ and *C/EBPα*$^{-/-}$ newborn mice femora (n = 5, repeated three times). (*C*) Quantification of bone volume/tissue volume and bone mineral density of *C/EBPα*$^{+/+}$ and *C/EBPα*$^{-/-}$ newborn mice femora. *P < 0.05; ***P < 0.001. (*D*) Histological sections of *C/EBPα*$^{-/-}$ newborn mice tibiae have an extended growth plates (arrows) and a dramatic reduction in TRAP^{+} OCs compared with *C/EBPα*$^{+/+}$ controls (n > 50). Boxed areas (*Upper*) are magnified (*Lower*). The histological sections of the same area of *C/EBPα*$^{-/-}$ newborn mice also show dramatically decreased TRAP^{+} OCs. (*E*) TRAP stain of RANKL-induced *C/EBPα*$^{+/+}$ and *C/EBPα*$^{-/-}$ MBM. (*F*) TRAP stain of cocultures with MOBs and MBM obtained from *C/EBPα*$^{-/-}$ and *C/EBPα*$^{+/+}$ mice.

Western blot analysis revealed that there are no major changes in the expression of NF-κB inhibitor, inhibitor of κBα (IκBα), and MAPK 14 (p38) or their phosphorylated forms (p-IκBα and p-p38) in *C/EBPα*$^{-/-}$ MBM cells cultured with M-CSF/RANKL for 0–60 min, compared with the C/*EBPα*$^{+/+}$ control (Fig. 4*C*). These data indicate that the role of *C/EBPα* in OCs

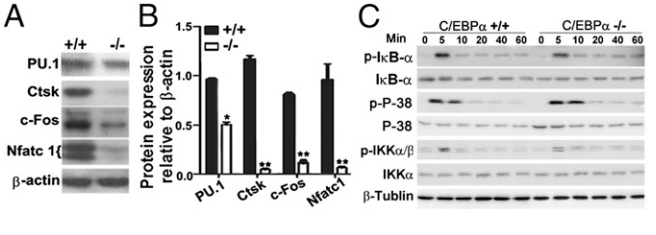

Fig. 4. *C/EBPα* KO reduces the expression of key OC regulators and marker genes. Western blot (*A*) and quantification of expression (*B*) of PU.1, Ctsk, c-Fos, and Nfatc1 in C/*EBPα*$^{+/+}$ and *C/EBPα*$^{-/-}$ MBM cells cultured with M-CSF (20 ng/mL) alone for 2 d and then stimulated with M-CSF (10 ng/mL)/RANKL (10 ng/mL) for 5 d to generate OC-like cells. *P < 0.05; **P < 0.01. (*C*) Time-course Western blot analysis of IκBα and p38 and their phosphorylated forms (p-IκBα and p-p38) in C/*EBPα*$^{+/+}$ and *C/EBPα*$^{-/-}$ MBM cells cultured with M-CSF (20 ng/mL) alone for 2 d and then stimulated with M-CSF (10 ng/mL)/RANKL (10 ng/mL) for 0–60 min.

does not involve the IκBα or p38 signaling pathways but that it may directly regulate the *c-fos* arm of the RANKL signaling pathways to promote osteoclastogenesis.

Both *C/EBPα*$^{-/-}$ and *C/EBPα*$^{+/-}$ Mice Exhibit an Increase in Trabecular Bone Numbers. To analyze the role of *C/EBPα* in bone homeostasis further, we stained *C/EBPα*$^{+/+}$ and *C/EBPα*$^{-/-}$ tibiae sections with Goldner's trichrome stain and performed histomorphometric analysis (using Bioquant software; BIOQUANT Image Analysis Corporation). Compared with *C/EBPα*$^{+/+}$ controls, *C/EBPα*$^{-/-}$ tibiae have growth plates with an extended zone of growth plate and a dramatic increase in mineralized tissue, which indicates osteopetrosis (Fig. 5*A*). Histomorphometric analysis revealed that KO of *C/EBPα* results in increased bone volume, distal and proximal hypertrophic growth plate thickness, and trabecular thickness (Fig. 5*B*). Our analyses also revealed that the ratio of OC surface to bone surface and the number of OCs per bone perimeter dramatically decreased in *C/EBPα*$^{-/-}$ tibiae compared with *C/EBPα*$^{+/+}$ tibiae (Fig. 5*B*), further confirming the important role of *C/EBPα* in osteoclastogenesis. To determine the importance of the *C/EBPα* dose in mature animals, we analyzed the bone phenotype in *C/EBPα*$^{+/-}$ mature mice.

Femora from heterozygous *C/EBPα*$^{+/-}$ mice (8 mo of age) exhibit an increase in bone density and an increase in trabecular bone compared with *C/EBPα*$^{+/+}$ controls (Fig. S3). Goldner's trichrome stain and histomorphometric analysis indicate that *C/EBPα*$^{+/-}$ femora have an increase in bone volume/tissue volume and trabecular number and a decrease in OC surface/bone surface and OC number/bone perimeter (Figs. S4 and S5).

***C/EBPα*$^{-/-}$ Impaired Osteoclastogenesis Is Rescued by Ectopic Expression of *c-fos*.** In order to confirm if *C/EBPα* regulates osteoclastogenesis through the *c-fos* arm of the RANKL signaling pathway, we next investigated whether ectopic expression of *c-fos* using retrovirus-mediated gene transfer could rescue the impaired OC differentiation caused by *C/EBPα* KO. MBM cells were stimulated with M-CSF/RANKL for OC differentiation analysis. These cultured *C/EBPα*$^{-/-}$ MBM cells were transduced by pBMN–*c-fos* or the control retrovirus pBMN-GFP (Fig. 5 *C* and *D*). Compared with the control, the number of multinucleated OCs present increased more than 20-fold when *c-fos* was overexpressed in cultured *C/EBPα*$^{-/-}$ myeloid cells (Fig. 5 *C* and *D*). This indicates that impaired OC differentiation caused by *C/EBPα* KO can be rescued by ectopic expression of *c-fos*.

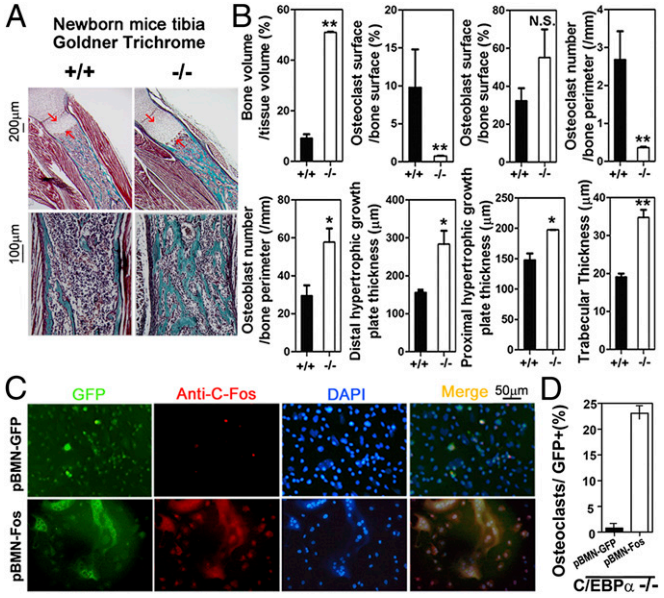

Fig. 5. *C/EBPα*$^{-/-}$ mice exhibit a dramatic increase in trabecular bone number, and *C/EBPα*$^{-/-}$ impaired osteoclastogenesis is rescued by ectopic expression of *c-fos*. (*A*) Compared with *C/EBPα*$^{+/+}$ controls, *C/EBPα*$^{-/-}$ tibiae have extended growth plates (arrows) and a dramatic increase in mineralized tissue (bright blue regions), which indicates osteopetrosis ($n = 3$, repeated three times). (*B*) Histomorphometric analysis of tibiae from *C/EBPα*$^{+/+}$ and *C/EBPα*$^{-/-}$ mice. *$P < 0.05$; **$P < 0.01$. N.S., not significant. (*C* and *D*) Impaired OC differentiation in *C/EBPα*$^{-/-}$ MBM cells cultured with M-CSF/RANKL can be rescued by ectopic expression of *c-fos* using pBMN–*c-fos* compared with control virus (pBMN-GFP). ***$P < 0.001$.

C/EBPα Induces Osteoclastogenesis in the Absence of RANKL and Activates the *c-fos* Promoter. To determine the mechanism of C/EBPα function in OC differentiation and gene expression further, we forced expression of C/EBPα in MBM cells by stimulating MBM with M-CSF alone (Fig. 6). To express C/EBPα in MBM ectopically, we constructed a retrovirus vector (pBMN-*C/EBPα*) that was engineered to express both *C/EBPα* and GFP. Then, MBM was transduced with the *C/EBPα*-expressing virus (pBMN-*C/EBPα*) or with a control virus (pBMN-GFP) as described (3). Western blot analysis demonstrates the effective retrovirus-mediated overexpression of C/EBPα in MBM stimulated with M-CSF alone for 96 h (Fig. 6*A*). The expression of *C/EBPα* increased significantly after 96 h of M-CSF stimulation (Fig. 6*A*). At the 96-h time point, there is a surprising marked increase in the number of TRAP$^+$ multinucleated OCs when *C/EBPα* is overexpressed compared with the control group even in the absence of RANKL stimulation. This underscores the important role of *C/EBPα* in osteoclastogenesis (Fig. 6*B*). Through qPCR, it was determined that the expression of markers common for macrophages and OCs (e.g., *RANK*, *Traf6*), key OC genes (e.g, *Nfatc1*, *c-fos*, *acid phosphatase 5 (Acp5)*, *matrix metallopeptidase 9 (Mmp9)*, *Ctsk),* and *C/EBPα* increased in the pBMN-C/EBPα transfected group (Fig. 6*C*). These data indicate that C/EBPα overexpression in the absence of RANKL stimulation can induce the formation of TRAP$^+$ multinucleated cells (Fig. 6 *B* and *C*). Because our results showed that overexpression of c-Fos can rescue the OC defect of C/EBPα$^{-/-}$ cells (Fig. 5*C*), it is important to determine if the c-fos promoter has C/EBPα binding sites. Accordingly, we performed ChIP assays with MBM stimulated with RANKL to generate mature OCs and found that C/EBPα directly binds regulatory sequences on the c-fos promoters (Fig. 6*D*) and activates c-fos expression (Fig. 6*E*). The truncated *c-fos* promoters were induced by C/EBPα, indicating the presence of two C/EBPα binding sites (Fig. 6*F*).

Ectopic Expression of C/EBPα Reprograms the Monocyte/Macrophage Cell Line to OC-Like Cells in the Absence of RANKL. To question whether ectopic expression of C/EBPα can reprogram the monocyte/macrophage cell line RAW264.7 cells to OC-like cells in the absence of RANKL, we ectopically expressed C/EBPα in RAW264.7 cells by using pcDNA3.1-*C/EBPα* or the vector control pcDNA3.1 (Fig. 7 *A*–*D*). Western blot analysis demonstrated the effective overexpression of C/EBPα by the plasmid stable transfection approach (Fig. 7*A*). Similarly, TRAP staining revealed that TRAP$^+$ OCs developed when *C/EBPα* was overexpressed in the absence of RANKL stimulation (Fig. 7*B*). In addition, Ctsk immunostaining demonstrated that *C/EBPα* overexpression in the absence of RANKL stimulation still resulted in the expression of the OC marker gene *Ctsk* (Fig. 7*B*). *C/EBPα* overexpression reduced the expression of F4/80, which is a macrophage marker gene. Semi-qPCR of *c-fos*, *Ctsk*, *Acp5*, and *Nfatc1* also demonstrated that *C/EBPα* overexpression increases the expression of key OC genes even in the absence of RANKL (Fig. 7*C*). We found that *C/EBPα* overexpression increased the expression of genes important for OC lineage commitment and differentiation (e.g., *Ctsk, PU.1, c-fos, CD115, Traf6, CD11b, Acp5, Nfatc1, Mmp9, Ppary, CD68, RANK*) (9) (Fig. 7*D*) through

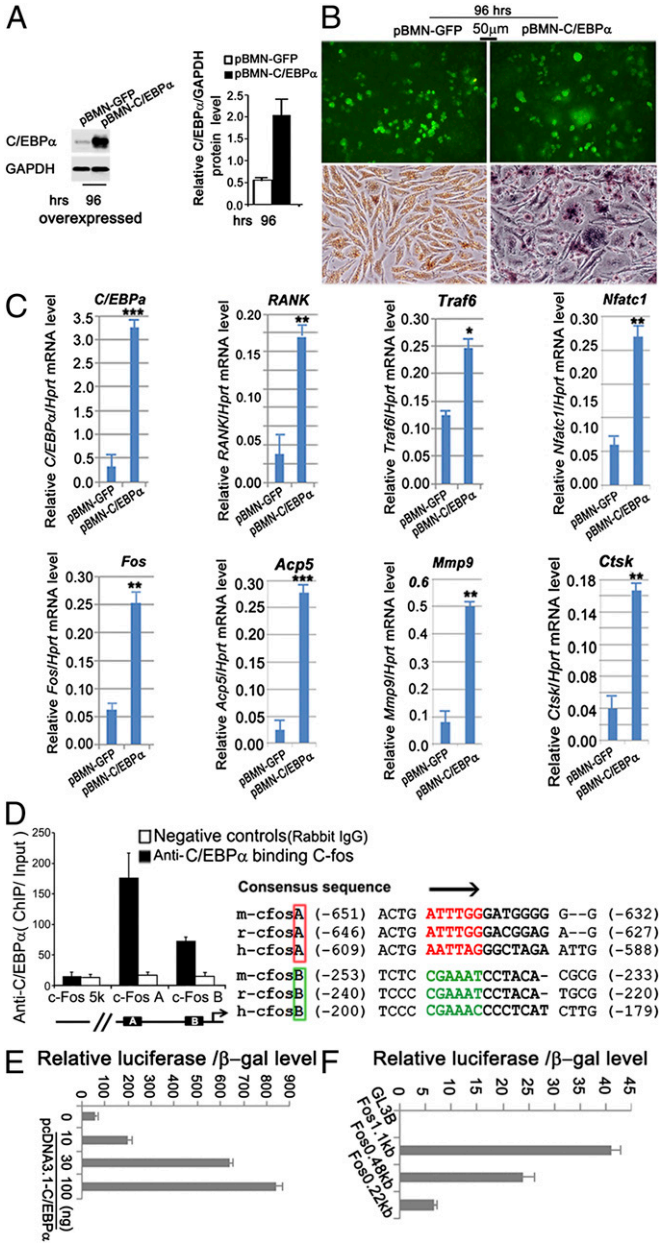

Fig. 6. C/EBPα induces osteoclastogenesis in the absence of RANKL and activates the *c-fos* promoter. (*A*) Western blot and quantification of forced expression of *C/EBPα* in *C/EBPα*$^{+/+}$ MBM stimulated with 20 ng/mL M-CSF for 24 h and then transduced with pBMN-C/EBPα for 96 h. Compared with the control group, C/EBPα expression increased significantly 96 h after cells were transduced with pBMN-C/EBPα. (*B*) GFP expression and TRAP expression in *C/EBPα*$^{+/+}$ MBM in which *C/EBPα* is overexpressed (pBMN-*C/EBPα*) compared with the control (pBMN-GFP) after 96 h of stimulation with M-CSF (20 ng/mL) alone. (*C*) qPCR analysis in MBM cultured in M-CSF alone and transduced with pBMN-*C/EBPα* (+) or with the vector control pBMN-GFP for 96 h. **P* < 0.05; ***P* < 0.01; ****P* < 0.001. (*D*) ChIP analysis of C/EBPα binding to the *c-fosA*, *c-fosB*, or upstream promoter region [*c-fos* (−5 Kb) as a negative control] in MBM stimulated with RANKL/M-CSF to generate mature OCs. (*E*) Consensus sequence alignment of putative C/EBPα binding sites of mouse, rat, and human *c-fos* promoter regions. C/EBPα activates c-Fos expression. (*F*) Truncated *c-fos* promoters were induced by C/EBPα. Luciferase reporter assays with truncated *c-fos* promoters indicated the presence of two C/EBPα binding sites (GL3B, control vector).

qPCR analysis of gene expression. Expression of *C/EBPβ* increased slightly when *C/EBPα* was overexpressed in uninduced RAW264.7 cells (Fig. 7*D*).

Discussion

In this study, we demonstrated that C/EBPα expression is essential for OC lineage commitment but that it may not be essential for macrophage differentiation. Importantly, forced expression of C/EBPα in MBM and RAW264.7 cells induced the expression of OC marker genes in the absence of RANKL stimulation (Figs. 6 and 7), which demonstrates that high expression of C/EBPα is sufficient for OC lineage commitment. This study filled the gap in our understanding of how transcription factor(s) specify OC lineage commitment from monocyte/macrophage cells.

C/EBPα Expression Is Essential for OC Lineage Commitment but May Not Be Essential for Macrophage Differentiation. We sought insight into the mechanism underlying C/EBPα's role in OC differentiation. Specifically, it is important to clarify if C/EBPα expression is important for OC lineage commitment alone or if it is also important for monocyte/macrophage differentiation because OCs are multinucleated cells derived from hematopoietic precursors of the monocyte/macrophage series. Feng et al. (19) discovered that the combined expression of *PU.1* and *C/EBPα* is sufficient to activate a myeloid program in fibroblasts, which are derived from mesenchymal stem cells, and to induce a macrophage-like phenotype. It has also been shown that enforced expression of *C/EBPα* and *C/EBPβ* in B cells leads to their rapid and efficient reprogramming into macrophages (20). Di Tullio et al. (21) recently clarified that this C/EBPα-induced transdifferentiation of pre-B cells into macrophages involves no overt retrodifferentiation. These studies indicate that C/EBPα is important for monocyte/macrophage differentiation. It has been determined that the loss of *C/EBPα* gene expression in hematopoietic progenitor cells results in a block in differentiation at the common myeloid progenitor and granulocyte/macrophage progenitor stage of development (22, 23), indicating that C/EBPα expression is important for the development of macrophage CFUs. There is some controversy regarding the requirement of

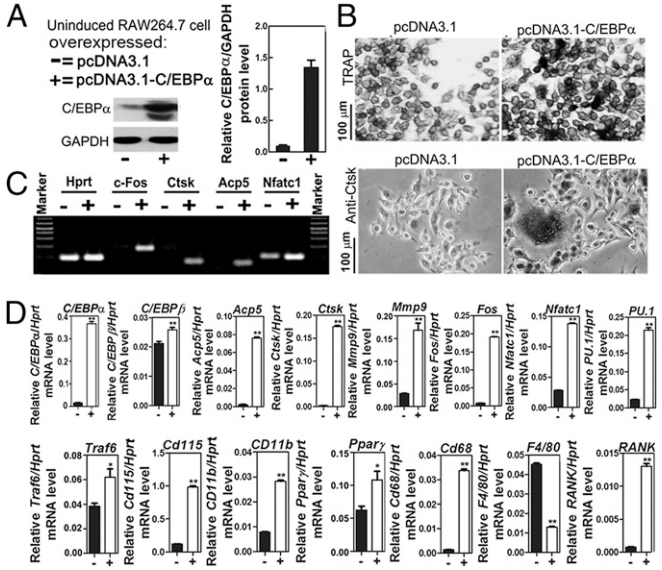

Fig. 7. Ectopic expression of C/EBPα reprograms the monocyte/macrophage cell line to OC-like cells in the absence of RANKL. (*A*) Western blot of C/EBPα expression in RAW264.7 cells (not stimulated with M-CSF/RANKL) transfected with pcDNA3.1-*C/EBPα* (+) or with the vector control pcDNA3.1 (−). (*B*) TRAP and Ctsk immunostaining in uninduced RAW264.7 cells in which *C/EBPα* is overexpressed [pcDNA3.1-*C/EBPα* (+)] compared with the control [pcDNA3.1 (−)]. Semi-qPCR (*C*) and qPCR (*D*) analysis (25 cycles, *Hprt* served as a loading control) of genes important for monocytes/macrophages and OCs in uninduced RAW264.7 cells transfected with pcDNA3.1-*C/EBPα* (+) or with the vector control pcDNA3.1 (−).**P* < 0.05; ***P* < 0.01.

C/EBPα for macrophage development (22, 23). Heath et al. (23) demonstrated that there was a defect in macrophage development in mice that received transplants of *C/EBPα*$^{-/-}$ fetal liver cells and that *C/EBPα*$^{-/-}$ fetal liver cells had decreased M-CSF receptor (Cd115). In contrast, Zhang et al. (22) determined that circulating blood and hematopoietic organs from *C/EBPα*$^{-/-}$ mice did not lack monocytes or macrophages and that there was no defect in the M-CSF receptor. Consistent with the study by Zhang et al. (22), our analysis of *C/EBPα*$^{-/-}$ fetal liver cells, *C/EBPα*$^{-/-}$ tibiae, and MBM-derived monocyte/macrophage cells indicates that *C/EBPα* is not essential for macrophage differentiation (Figs. S6–S8). These contrasting results are likely due to differences in the experimental systems utilized, such as *C/EBPα*$^{-/-}$ mice and mice transplanted with *C/EBPα*$^{-/-}$ fetal liver cells.

C/EBPα Is a Major Regulator of OC Lineage Commitment but Is Not Sufficient for Terminal OC Differentiation. *C-fos* functions downstream of RANKL signaling and plays an essential function in the developmental stage from monocyte/macrophage precursors to mature OCs (5). *C-fos* is also important for the expression of Nfactc1, which is a regulator of terminal differentiation of OCs (3). Importantly, forced expression of C/EBPα, even in the absence of RANKL stimulation, induced the expression of these key OC transcription factors (e.g., *c-fos*, *Nfatc1*) and *PU.1* (24) (Fig. 6). Our data indicate that *C/EBPα* may directly regulate *c-fos* to promote osteoclastogenesis. We determined that the *c-fos* promoter has two C/EBPα binding sites (Fig. 6*D*) and that C/EBPα may activate the *c-fos* promoter through the two C/EBPα binding sites (Fig 6 *E* and *F*). Notably, our results indicate that C/EBPα modulates both OC lineage commitment and terminal OC differentiation. Indeed, C/EBPα binding sites are present at both the c-fos promoter and the Ctsk promoter, the latter of which is a gene expressed by committed OCs. In addition, ectopic expression of C/EBPα induces upregulation of both early and late OC markers. Thus, these findings demonstrate that high expression of C/EBPα alone is sufficient for OC lineage commitment and that C/EBPα also modulates terminal OC differentiation.

Potential Mechanism Underlying C/EBPα Is Induced by RANKL. How C/EBPα is induced by RANKL is unclear. However, NF-κB, which is induced by RANKL, regulates C/EBPα expression in myeloid cells. It is thus possible that RANKL induces NF-κB expression, which, in turn, activates C/EBPα expression. It was noted that C/EBPα overexpression largely increased RANK (RANKL receptor) expression (Figs. 6*C* and 7*D*). Thus, another way that C/EBPα may be induced by RANKL (ligand) is through a self-amplification pathway. We suspect that C/EBPα upregulates the expression of receptor RANK, which allows for increased binding of RANKL and triggers the cascade of transcription factors specifying OC lineage commitment.

Importantly, our research indicates that a threshold level of C/EBPα expression is an important component in the mechanism by which M-CSF acts with RANKL to promote OC differentiation, whereas it promotes macrophage differentiation when it acts alone. Thus, this study provides essential insight into the long-standing question of how RANKL promotes OC differentiation. These findings expand the existing view of the role of C/EBPα in bone homeostasis beyond its role in lineage allocation of mesenchymal stem cells and macrophage cells to include a direct and specific role in OC lineage commitment from monocyte/macrophage cells. C/EBPα may be an ideal target for treating osteolytic diseases.

Materials and Methods

***Ctsk* Promoter CAT Constructs.** A *Ctsk* pCCAT containing a 1,505-bp XbaI/EcoRI fragment (−1,474 to −31, numbered relative to the cap site) of the mouse *Ctsk* 5′-flanking region was used as a starting point for deletion analysis. The sizes of series of 5′ deletions generated were approximated by electrophoresis in a 3:1 NuSieve-agarose gel (Lonza) or, in selected cases, by DNA sequence analysis with the dideoxy chain termination method.

Forced Expression. We used a retrovirus system to express *c-fos* ectopically, as described previously (17), in *C/EBPα*$^{-/-}$ myeloid cells cultured with M-CSF/RANKL to induce osteoclastogenesis. We similarly used a retrovirus system to express *C/EBPα* ectopically in RANKL-induced C/EBP$\alpha^{+/+}$ MBM as described previously (17). *C/EBPα* was also overexpressed in uninduced RAW264.7 cells by stable transfection.

Statistical Analysis and Data Quantification Analysis. Experimental data are reported as mean ± SD of triplicate independent samples. Data were analyzed with the two-tailed Student's *t* test. *P* values <0.05 were considered significant. Data quantification analyses were performed using the National Institutes of Health ImageJ program as described (12, 17) (*$P < 0.05$ and **$P < 0.01$ throughout the paper). Additional details are provided in *SI Materials and Methods*.

ACKNOWLEDGMENTS. We thank Ms. Christie Paulson for her excellent assistance with our manuscript and Dr. Jay M. McDonald for his extensive reading and discussion of our manuscript. We also thank Dr. Yihong Wan for the generous gift of *c-fos* promoter luciferase constructs, Dr. Gretchen J. Darlington (Baylor College of Medicine, Houston) for the generous gift of *C/EBPα*$^{+/-}$ mice, and Matthew McConnell for his assistance with bioinformatics analysis. We appreciate the assistance of the Center for Metabolic Bone Disease at the University of Alabama at Birmingham (Grant P30 AR046031). We are also grateful for assistance from the Small Animal Phenotyping Core, Metabolism Core, and Neuroscience Molecular Detection Core Laboratory at the University of Alabama at Birmingham (Grant P30 NS0474666). This work was supported by National Institutes of Health Grants AR-44741 and AR-055307 (both to Y.-P.L.).

1. Valledor AF, Borràs FE, Cullell-Young M, Celada A (1998) Transcription factors that regulate monocyte/macrophage differentiation. *J Leukoc Biol* 63(4):405–417.
2. Zhao B, Ivashkiv LB (2011) Negative regulation of osteoclastogenesis and bone resorption by cytokines and transcriptional repressors. *Arthritis Res Ther* 13(4):234.
3. Takayanagi H, et al. (2002) Induction and activation of the transcription factor NFATc1 (NFAT2) integrate RANKL signaling in terminal differentiation of osteoclasts. *Dev Cell* 3(6):889–901.
4. Iotsova V, et al. (1997) Osteopetrosis in mice lacking NF-kappaB1 and NF-kappaB2. *Nat Med* 3(11):1285–1289.
5. Grigoriadis AE, et al. (1994) c-Fos: A key regulator of osteoclast-macrophage lineage determination and bone remodeling. *Science* 266(5184):443–448.
6. Braun T, Zwerina J (2011) Positive regulators of osteoclastogenesis and bone resorption in rheumatoid arthritis. *Arthritis Res Ther* 13(4):235.
7. Nakashima T, Takayanagi H (2011) New regulation mechanisms of osteoclast differentiation. *Ann N Y Acad Sci* 1240:E13–E18.
8. Tondravi MM, et al. (1997) Osteopetrosis in mice lacking haematopoietic transcription factor PU.1. *Nature* 386(6620):81–84.
9. Wan Y, Chong LW, Evans RM (2007) PPAR-gamma regulates osteoclastogenesis in mice. *Nat Med* 13(12):1496–1503.
10. Sharma SM, et al. (2006) Genetics and genomics of osteoclast differentiation: Integrating cell signaling pathways and gene networks. *Crit Rev Eukaryot Gene Expr* 16(3):253–277.
11. Li YP, et al. (1995) Cloning and complete coding sequence of a novel human cathepsin expressed in giant cells of osteoclastomas. *J Bone Miner Res* 10(8):1197–1202.
12. Chen W, et al. (2007) Novel pycnodysostosis mouse model uncovers cathepsin K function as a potential regulator of osteoclast apoptosis and senescence. *Hum Mol Genet* 16(4):410–423.
13. Schepers H, et al. (2007) Reintroduction of C/EBPalpha in leukemic CD34+ stem/progenitor cells impairs self-renewal and partially restores myelopoiesis. *Blood* 110(4):1317–1325.
14. Cammenga J, et al. (2003) Induction of C/EBPalpha activity alters gene expression and differentiation of human CD34+ cells. *Blood* 101(6):2206–2214.
15. Friedman AD (2007) Transcriptional control of granulocyte and monocyte development. *Oncogene* 26(47):6816–6828.
16. Koleva RI, et al. (2012) C/EBPα and DEK coordinately regulate myeloid differentiation. *Blood* 119(21):4878–4888.
17. Yang S, Li YP (2007) RGS10-null mutation impairs osteoclast differentiation resulting from the loss of [Ca2+]i oscillation regulation. *Genes Dev* 21(14):1803–1816.
18. Li YP, Chen W, Liang Y, Li E, Stashenko P (1999) Atp6i-deficient mice exhibit severe osteopetrosis due to loss of osteoclast-mediated extracellular acidification. *Nat Genet* 23(4):447–451.
19. Feng R, et al. (2008) PU.1 and C/EBPalpha/beta convert fibroblasts into macrophage-like cells. *Proc Natl Acad Sci USA* 105(16):6057–6062.
20. Xie H, Ye M, Feng R, Graf T (2004) Stepwise reprogramming of B cells into macrophages. *Cell* 117(5):663–676.
21. Di Tullio A, et al. (2011) CCAAT/enhancer binding protein alpha (C/EBP(alpha))-induced transdifferentiation of pre-B cells into macrophages involves no overt retrodifferentiation. *Proc Natl Acad Sci USA* 108(41):17016–17021.
22. Zhang DE, et al. (1997) Absence of granulocyte colony-stimulating factor signaling and neutrophil development in CCAAT enhancer binding protein alpha-deficient mice. *Proc Natl Acad Sci USA* 94(2):569–574.
23. Heath V, et al. (2004) C/EBPalpha deficiency results in hyperproliferation of hematopoietic progenitor cells and disrupts macrophage development in vitro and in vivo. *Blood* 104(6):1639–1647.
24. Teitelbaum SL, Ross FP (2003) Genetic regulation of osteoclast development and function. *Nat Rev Genet* 4(8):638–649.

Supporting Information

Chen et al. 10.1073/pnas.1211383110

SI Materials and Methods

Animal Experimentation. All animal experimentation was carried out according to the legal requirements of the Association for Assessment and Accreditation of the Laboratory Animal Care International and the University of Alabama at Birmingham Institutional Animal Care and Use Committee. We used *CCAAT/enhancer binding protein α double-negative* (*C/EBPα*$^{-/-}$) mice, which were a gift from Gretchen J. Darlington (1). Heterozygous C/EBPα$^{+/-}$ male mice were crossed with C/EBPα$^{+/-}$ female mice to obtain C/EBPα$^{-/-}$ and C/EBPα$^{+/+}$ (control) mice. Mice were bred in-house and killed by CO_2 asphyxiation. Samples of organs and tissues were obtained from newborn mice, including mouse bone marrow (MBM), bone, brain, kidney, liver, and muscle.

Cells and Cell Culture. Mature osteoclasts (OCs) in primary culture were generated from MBM as described (2–4). Briefly, MBM was obtained from the tibiae and femora of 6-wk-old female WT *C/EBPα*$^{+/+}$ mice as described (5, 6). Although constitutive *C/EBPα* deletion results in mortality within a few hours of birth (1), we were able to extract MBM from newborn *C/EBPα*$^{+/+}$ and *C/EBPα*$^{-/-}$ mice. Some MBM cells ($1–2 \times 10^5$) were seeded into the wells of a 24-well plate, and other MBM cells (1×10^6) were seeded into the wells of 6-well plate. MBM cells were cultured in α-modified MEM (GIBCO-BRL) with 10% (vol/vol) FBS (GIBCO-BRL) containing 20 ng/mL macrophage colony-stimulating factor (M-CSF; R&D Systems). After 24 h, cells were cultured in the presence of 10 ng/mL receptor activator of NF-κB ligand (RANKL; R&D Systems) and 10 ng/mL M-CSF for an additional 96 h to generate OCs.

To generate mature OCs from the coculture system, MBM and calvarial osteoblasts from *C/EBPα*$^{+/+}$ and *C/EBPα*$^{-/-}$ mice were cultured in the presence of 10^{-8} M $1,25(OH)_2$ vitamin D_3 and 10^{-6} M dexamethasone as described previously (7). Primary calvarial osteoblasts were isolated from C/*EBPα*$^{+/+}$ and *C/EBPα*$^{-/-}$ mice on postnatal day 1 as we previously described (7).

C/EBPα$^{+/+}$ and *C/EBPα*$^{-/-}$ spleen cells were cultured with M-CSF (20 ng/mL) alone for 48 h and were then stimulated with M-CSF (10 ng/mL)/RANKL (10 ng/mL) to generate OC-like cells as we previously described (4, 7–9). Alternatively, spleen cells were stimulated with 20 ng/mL M-CSF alone to generate monocyte/macrophage-like cells as described previously (4, 7–9).

C/EBPα$^{+/+}$ and *C/EBPα*$^{-/-}$ livers were harvested on embryonic days 17.5–18 and cut to small pieces and lysised with 0.05% 1X trypsin/EDTA (Invitrogen) to harvest single cells. Harvested single cells were reseeded in culture dishes and cultured with RANKL/M-CSF as described above to induce OC differentiation. The mouse OC precursor cell line RAW264.7 obtained from the American Type Culture Collection was treated with M-CSF/RANKL to induce OC differentiation as we previously described (4).

Rat osteoblast cells were derived from calvaria as described previously (7). Giant cell tumors (GCTs) of bone contain human stromal cells (hSCs), OC-like precursors, and OC-like giant cells. Because OC-like giant cells from GCTs of bone are effectively the same as OCs in bone, we used GCTs and hSCs obtained from GCTs as previously described (10). The human macrophage (U-937) cell line was purchased from the American Type Culture Collection.

***Cathepsin K* Promoter CAT Constructs.** We characterized the *Cathepsin K* (*Ctsk*) promoter as described (11). The XbaI/EcoRI fragment was subcloned into a pBluescript KS vector (Stratagene) and digested with KpnI/SmaI before insertion of the gene-vector fragment into pCAT-3 Basic Reporter Vector (Promega) to produce pCCAT-1474. The pCCAT-1474 was digested with KpnI and EcoRV, and the product was subjected to controlled 5′ → 3′ digestion with exonuclease III using Erase-a-Base Systems (Promega). The sizes of series of 5′ deletions generated were approximated by electrophoresis in a 3:1 NuSieve-agarose gel (Lonza) or, in selected cases, by DNA sequence analysis with the dideoxy chain termination method.

Cell Transfection and CAT Assay. To determine 5′-flanking regulatory activity, constructs were transfected into RANKL-induced RAW264.7 cells using lipofectamine reagent (BRL) as described (12). The transfected RAW264.7 cells induced to OCs were tested for differential expression of CAT activity as described (13). CAT activity in transfected cultures is standardized by normalization to β-gal activity and the protein concentration of cell extracts using a protein assay kit (BioRad) as described (10, 14). In all experiments, constructs were tested in duplicate or triplicate.

Site-Directed Mutagenesis. Site-directed mutant constructs were created as previously described (10, 14). In brief, a SpeI restriction site was introduced into pCCAT-137 in the mutant fusion gene as indicated in Fig. 1*B*. The SpeI fragment from the mutant gene was isolated and cloned into the identical site in pCCAT-137.

Electrophoretic Mobility Shift Assay. Nuclear extracts were prepared as previously described (15). Gel retardation assays were carried out as described with slight modification (10, 14). For the electrophoretic mobility shift assay, double-stranded oligonucleotides encoding the −53 to −30 region of the *Ctsk* promoter were end-labeled with ^{32}P and used as probes. Competition experiments were performed with a mixture of nuclear extract, and the ^{32}P-labeled −53 to −30 WT *Ctsk* promoter oligonucleotide probe was incubated with unlabeled competitors (e.g., −53 to −30 WT *Ctsk* promoter oligonucleotide, mutant oligonucleotides, activator protein-1 oligonucleotide). Ten mutant oligonucleotides (shown in Fig. 1*D*) were synthesized with 2-bp substitutions of the −53 to −30 WT *Ctsk* promoter sequence AGTTGACTTCCG-CAATCCTTACCG. Mixtures were incubated for 20 min on ice, loaded onto a 4% (vol/vol) nondenaturing polyacrylamide gel, and subjected to electrophoresis. Supershift mobility assays were carried out with antibodies against C/*EBPα,* C/*EBPβ*, or C/*EBPδ* (Santa Cruz Biotechnology) in order to define the factor that binds the critical *cis*-regulatory element recognition site.

DNase I Footprint Analysis. We performed a DNase I footprint analysis as previously described (14). Nuclear extracts from RANKL-induced RAW264.7 cells were prepared by the method of Dignam et al. (16). A 234-bp probe was prepared by PCR assay. The PCR product was purified with the Magic PCR Preps DNA purification system (Promega) and was end-labeled with ^{32}P. The labeled PCR product was digested with DNase I restriction endonuclease. Approximately 104 cpm of end-labeled, polyacrylamide gel-purified probe was incubated with RANKL-induced RAW264.7 cell nuclear extracts for 15 min on ice and then for 2 min at 25 °C. DNase I (1 U/mL) was added for 1 min at 25 °C and separated on an 8% (vol/vol) sequencing gel.

Northern Blotting Analysis. Northern blotting was performed as described previously (10, 17). Total RNA (15 μg per lane) was isolated using TRIzol reagent (Life Technologies) (4). Human

C/*EBPα* transcript (2.4 kb) and mouse C/*EBPα* transcript (2.7 kb) were used as C/*EBPα*-cDNA probes. Blots were stripped and rehybridized with 28S and GAPDH cDNA for normalization purposes.

Western Blotting Analysis. Western blotting was performed as described (4, 17) and visualized and quantified using a Fluor-S Multi-Imager and Multi-Analyst software (Bio-Rad). We used rabbit anti-Ctsk polyclonal antibody, which was previously generated in our laboratory (11). We also used antibodies for C/EBPα, proviral integration 1 (PU.1), Finkel-Biskis-Jinkins osteosarcoma oncogene (*c-fos*), and nuclear factor of activated T cells cytoplasmic 1 (NFATc1) purchased from Santa Cruz Biotechnology. We performed a time-course Western blot analysis using antibodies for inhibitor of κBα (IκBα), phosphorylated (p)-IκBα, p38, p-p38, Iκκα, and p-Iκκαβ (Cell Signaling) in C/*EBPα*$^{+/+}$ and C/*EBPα*$^{-/-}$ MBM cells cultured with M-CSF/RANKL for 0–60 min. We also performed a time-course Western blot analysis of C/EBPα expression in MBM after 0–120 h of M-CSF/RANKL induction. β-actin, GAPDH, and β-tubulin were used as controls.

Histological and Radiographic Procedures. Histological analyses were performed as described ($n > 50$) (7). TNF receptor-associated protein 1 (TRAP) was used as a marker for OCs using a commercial kit (Sigma) according to the manufacturer's instructions. Multinucleated (more than three nuclei) TRAP$^+$ cells appear as dark purple cells and were counted by light microscopy ($n > 50$). Tibiae from C/*EBPα*$^{+/+}$ and C/*EBPα*$^{-/-}$ mice were stained with Goldner's trichrome ($n = 3$); bright blue regions indicate mineralized tissue. For X-ray analysis, radiography was performed using a high-resolution soft X-ray system at 30 kV and high-speed holographic film (Kodak) ($n = 5$). Microcomputed tomography analysis was performed to determine the bone mass of fixed femora as described (18) by the University of Alabama at Birmingham Small Animal Bone Phenotyping Core associated with the Center for Metabolic Bone Disease ($n = 3$).

Immunostaining. Immunostaining was carried out as described (4). Two specific antibodies, F4/80 (Biosource International) and CD11b (Pharmingen), were used as markers of monocyte/macrophage precursors as described previously ($n > 9$) (12, 19). In addition, we used antibodies for C/EBPα, C/EBPβ, and C/EBPδ purchased from Santa Cruz Biotechnology, as well as antibodies for Ctsk as described above.

Immunofluorescence Analysis. We performed immunofluorescence analysis as we have previously described (3), with the exception that we used anti-C/EBPα and anti-Ctsk as the primary antibodies purchased from Santa Cruz Biotechnology, and observations were performed by epifluorescence in a Zeiss axioplan microscope in the Developmental Neurobiology Imaging and Tissue Processing Core at the University of Alabama at Birmingham Intellectual and Disabilities Research Center. Nuclei were visualized with 1 μg/mL DAPI (Sigma). To visualize filamentous (F-actin) rings, MBM was stained with 2 U/mL Alexa Fluor 546-phalloidin (Molecular Probes) as previously described (20). The experiments were set in triplicate on three independent occasions.

Real-Time Quantitative PCR and Semiquantitative PCR. Real-time (RT) quantitative PCR (qPCR) was performed as described (21, 22) using TaqMan probes purchased from Applied Biosystems as listed in Table S1. Briefly, cDNA fragments were amplified by TaqMan Fast Advanced Master Mix (Applied Biosystems). Fluorescence from each TaqMan probe was detected by a Step-One RT-PCR system (Applied Biosystems). RNA samples were obtained from transduced MBM cultured with M-CSF alone, MBM-derived OC-like cells, MBM-derived monocyte/macrophage-like cells, or transfected uninduced RAW264.7 cells. The mRNA expression level of the housekeeping gene *hypoxanthine-guanine phosphoribosyl transferase* (*Hprt*) was used as an endogenous control and enabled calculation of specific mRNA expression levels as a ratio of *Hprt*. Primer sequences used for semi-qPCR are listed in Table S1. PCR conditions are available on request. Experiments were repeated at least three times.

Histomorphometric Analysis. Histomorphometric samples were processed as non-decalcified hard-tissue sections as described (7, 8). Briefly, for quantitative bone volume histomorphometry, 5-μm sections of newborn C/*EBPα*$^{-/-}$ and C/*EBPα*$^{+/+}$ mice were stained with Goldner's trichrome. For histomorphometric analysis of OC size and number, 10-μm sections of newborn C/EBPα$^{-/-}$ and C/EBPα$^{+/+}$ mice were TRAP-stained without counterstaining. Histomorphometric analysis of these sections was performed using the National Institutes of Health ImageJ program. Eight parameters studied in this analysis are presented: bone volume relative to tissue volume, the percentage of OC surface area to total bone surface area of the tibiae, the percentage of osteoblast surface area to total bone surface area of the tibiae, OC numbers per bone perimeter, osteoblast numbers per bone perimeter, distal hypertrophic growth plate thickness, proximal hypertrophic growth plate thickness, and trabecular thickness. Large multinucleated cells with cytoplasmic vesicles and intimate contact to bone were considered as OCs, and cuboidal mononuclear cells in intimate contact with osteoid or bone were identified as osteoblasts.

Flow Cytometry. Alexa Fluor 488-conjugated anti-mouse F4/80 antigen antibody for flow cytometry was purchased from eBioscience. Cells were washed in ice-cold flow cytometry buffer [2% (vol/vol) FCS and 2 mM EDTA in PBS, pH 7.5] and then incubated with antibody for 15 min and washed twice with flow cytometry buffer. Cells were fixed with 4% (wt/vol) paraformaldehyde before acquiring data using a FACSCalibur flow cytometer (BD Biosciences) and performing analysis with FlowJo (TreeStar).

Forced Expression. MBM cells (5×10^5) were seeded into the wells of a 12-well plate (without blood cells) and stimulated with 20 ng/mL M-CSF for 24 h. The attached cell number was confirmed to 60–70% of the total cell number. We used a retrovirus system to express *C/EBPα* ectopically in M-CSF–induced C/*EBPα*$^{+/+}$ MBM cells as described (7). We constructed a retrovirus vector (pBMN-*C/EBPα*) that was engineered to express both *C/EBPα* and GFP. The mouse C/EBPα cDNA was amplified and cloned into the pBMN retroviral vector (purchased from Addgene). We achieved retrovirus packaging by transducing pBMN into phoenix cells using the phoenix independent helper system. The viral supernatant was collected 52 h later. MBM cells were then transduced with the *C/EBPα*-expressing virus (pBMN-*C/EBPα*) or with a control virus (pBMN-GFP) overnight at 37 °C as described (19) and stimulated with 20 ng/mL M-CSF for 24 h. Medium was replaced with fresh α-MEM with 10% (vol/vol) FBS and additionally stimulated with 20 ng/mL M-CSF for 96 h.

We similarly used a retrovirus system to express *c-fos* ectopically, as described previously (7), in C/*EBPα*$^{-/-}$ myeloid cells cultured with M-CSF/RANKL to induce osteoclastogenesis. We then quantified the number of multinucleated OCs as a percentage of the number of GFP$^+$ cells as described (7, 23).

C/EBPα was also overexpressed in uninduced RAW264.7 cells by plasmid stable transfection as described (12, 14). *C/EBPα* cDNA (full-length cDNA from Open Biosystems) was cloned into the pCDNA3.1 expression vector (Invitrogen). RAW264.7 cells were transfected with pcDNA3.1-C/*EBPα* or with the vector control pcDNA3.1. RAW264.7 cells carrying pcDNA3.1-C/*EBPα* or the vector control pcDNA3.1 were passaged three times.

Promoter Analyses. For *c-fos* promoter luciferase promoter analyses, we used RAW264.7 cells maintained in DMEM high glucose containing 10% (vol/vol) FBS. Cells were cotransfected with increasing amounts of pcDNA3.1 (+) C/EBPα (0, 10, 30, or 100 ng per well), pSV-β-Galactosidase control vector (Promega) (50 ng per well), and GL3B, *c-fos* 1.1 kb, *c-fos* 0.48 kb, or *c-fos* 0.22 kb (50 ng per well) using the Lipofectamine transfection 2000 reagent (Invitrogen) and incubated for 6–8 h. Culture medium was replaced with fresh 10% (vol/vol) DMEM with M-CSF (10 ng/mL) and RANKL (10 ng/mL) and cultured for 3 d. Luciferase activity was measured using a Steady-Glo luciferase assay system (Promega). PGL3 basic reporter vectors were used as controls (Promega). Luminescence was detected with a luminometer (BioTek Synergy 2). For ChIP analyses, MBM-derived monocytes and macrophages were differentiated in M-CSF (20 ng/mL) for 24 h. Cells were further cultured for an additional 96 h in the presence of M-CSF (10 ng/mL)/RANKL (10 ng/mL) and C/EBPα-specific antibodies (Santa Cruz Biotechnology). The output of ChIP assays was measured by qPCR and normalized by 10% (vol/vol) input. All assays were repeated at least three times.

1. Wang ND, et al. (1995) Impaired energy homeostasis in C/EBP alpha knockout mice. *Science* 269(5227):1108–1112.
2. Yang S, Li YP (2007) RGS12 is essential for RANKL-evoked signaling for terminal differentiation of osteoclasts in vitro. *J Bone Miner Res* 22(1):45–54.
3. Feng S, et al. (2009) Atp6v1c1 is an essential component of the osteoclast proton pump and in F-actin ring formation in osteoclasts. *Biochem J* 417(1):195–203.
4. Yang S, Chen W, Stashenko P, Li YP (2007) Specificity of RGS10A as a key component in the RANKL signaling mechanism for osteoclast differentiation. *J Cell Sci* 120(Pt 19): 3362–3371.
5. Kelly KA, Tanaka S, Baron R, Gimble JM (1998) Murine bone marrow stromally derived BMS2 adipocytes support differentiation and function of osteoclast-like cells in vitro. *Endocrinology* 139(4):2092–2101.
6. Kurland JI, Kincade PW, Moore MA (1977) Regulation of B-lymphocyte clonal proliferation by stimulatory and inhibitory macrophage-derived factors. *J Exp Med* 146(5):1420–1435.
7. Yang S, Li YP (2007) RGS10-null mutation impairs osteoclast differentiation resulting from the loss of [Ca2+]i oscillation regulation. *Genes Dev* 21(14):1803–1816.
8. Chen W, et al. (2007) Novel pycnodysostosis mouse model uncovers cathepsin K function as a potential regulator of osteoclast apoptosis and senescence. *Hum Mol Genet* 16(4):410–423.
9. Li YP, Chen W, Liang Y, Li E, Stashenko P (1999) Atp6i-deficient mice exhibit severe osteopetrosis due to loss of osteoclast-mediated extracellular acidification. *Nat Genet* 23(4):447–451.
10. Li YP, et al. (1995) Cloning and complete coding sequence of a novel human cathepsin expressed in giant cells of osteoclastomas. *J Bone Miner Res* 10(8):1197–1202.
11. Li YP, Chen W (1999) Characterization of mouse cathepsin K gene, the gene promoter, and the gene expression. *J Bone Miner Res* 14(4):487–499.
12. Chen W, Li YP (1998) Generation of mouse osteoclastogenic cell lines immortalized with SV40 large T antigen. *J Bone Miner Res* 13(7):1112–1123.
13. Neumann JR, Morency CA, Russian KO (1987) A novel rapid assay for chloramphenicol acetyltransferase gene expression. *Biotechniques* 5(5):444–447.
14. Li YP, Stashenko P (1993) Characterization of a tumor necrosis factor-responsive element which down-regulates the human osteocalcin gene. *Mol Cell Biol* 13(6): 3714–3721.
15. Deryckere F, Gannon F (1994) A one-hour minipreparation technique for extraction of DNA-binding proteins from animal tissues. *Biotechniques* 16(3):405.
16. Dignam JD, Martin PL, Shastry BS, Roeder RG (1983) Eukaryotic gene transcription with purified components. *Methods Enzymol* 101:582–598.
17. Yang S, et al. (2003) In vitro and in vivo synergistic interactions between the Runx2/Cbfa1 transcription factor and bone morphogenetic protein-2 in stimulating osteoblast differentiation. *J Bone Miner Res* 18(4):705–715.
18. Rüegsegger P, Koller B, Müller R (1996) A microtomographic system for the nondestructive evaluation of bone architecture. *Calcif Tissue Int* 58(1):24–29.
19. Takayanagi H, et al. (2002) Induction and activation of the transcription factor NFATc1 (NFAT2) integrate RANKL signaling in terminal differentiation of osteoclasts. *Dev Cell* 3(6):889–901.
20. Wu H, Xu G, Li YP (2009) Atp6v0d2 is an essential component of the osteoclast-specific proton pump that mediates extracellular acidification in bone resorption. *J Bone Miner Res* 24(5):871–885.
21. Allaire JM, et al. (2011) Loss of Smad5 leads to the disassembly of the apical junctional complex and increased susceptibility to experimental colitis. *Am J Physiol Gastrointest Liver Physiol* 300(4):G586–G597.
22. Nijenhuis T, et al. (2008) Bone resorption inhibitor alendronate normalizes the reduced bone thickness of TRPV5(-/-) mice. *J Bone Miner Res* 23(11):1815–1824.
23. Wan Y, Chong LW, Evans RM (2007) PPAR-gamma regulates osteoclastogenesis in mice. *Nat Med* 13(12):1496–1503.

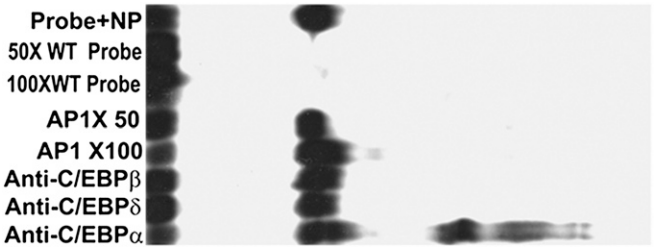

Fig. S1. *Ctsk* critical *cis*-regulatory element (CCRE) contains a specific protein complex binding site that only binds to OC-like cell nuclear proteins (NPs). A gel mobility shift experiment was conducted using a 0- to 100-fold molar excess of ^{32}P-labeled −53 to −30 WT *Ctsk* promoter oligonucleotide probe in nuclear extracts prepared from RANKL-induced RAW264.7 cells. The WT *Ctsk* probe and RANKL-induced RAW264.7 cell nuclear extracts were incubated with unlabeled activator protein 1 (AP-1) at a 50- or 100-fold molar excess. The WT *Ctsk* probe and RANKL-induced RAW264.7 cell nuclear extracts were incubated with antibodies against C/EBPβ, C/EBPδ, or C/EBPα.

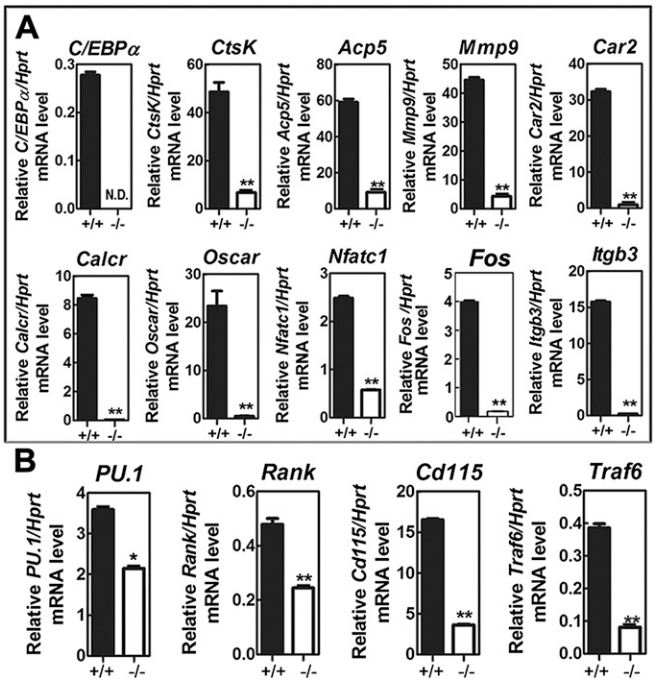

Fig. S2. *C/EBPα* is essential for the induction of OC-specific genes but not essential for the induction of macrophage-specific genes. (*A*) RT-qPCR assay of genes important for osteoclastogenesis and OC-specific functional genes in MBM cells cultured with M-CSF/RANKL. KO of *C/EBPα* dramatically reduced the expression of both RANKL-induced OC transcription factors [*c-fos* and nuclear factor of activated cells cytoplasmic 1 (*Nfatc1*)]. *Acp5, tartrate-resistant acid phosphatase; Calcr, calcitonin receptor; Car2, carbonic anhydrase 2; Itgb3, integrin beta 3; Mmp9, matrix metallopeptidase 9;* N.D., not detected; *Oscar, osteoclast associated receptor*. (*B*) RT-qPCR assay of genes common to both macrophages and OCs in MBM cells cultured with M-CSF/RANKL. KO of *C/EBPα* resulted in a relatively less severe decrease in the expression of genes that are common to macrophages and OCs, including transcription factor *SFFV proviral integration 1 (PU.1), receptor activator of NF-κB* (*RANK*), *colony stimulating factor 1 receptor (CD115 or M-CSF receptor*), and *TNF receptor-associated factor 6* (*Traf6*). $*P < 0.05$; $**P < 0.01$.

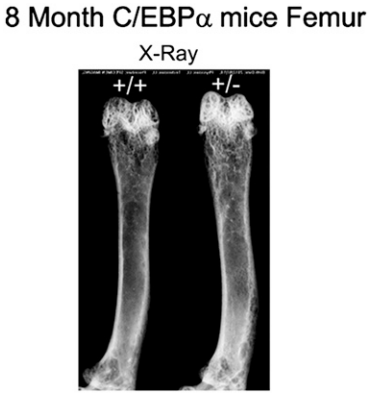

Fig. S3. Heterozygous $C/EBP\alpha^{+/-}$ femora exhibit increased bone density. X-ray analysis of femora indicates increased bone density in 8-mo-old $C/EBP\alpha^{+/-}$ mice compared with $C/EBP\alpha^{+/+}$ mice of the same age ($n = 3$, repeated three times).

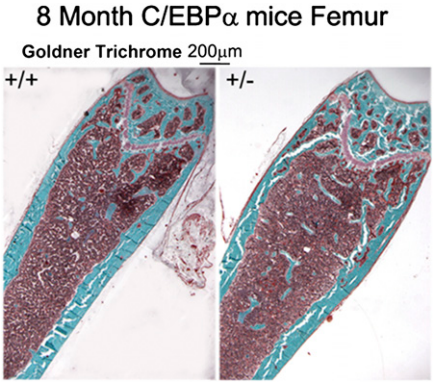

Fig. S4. Heterozygous *C/EBPα*$^{+/-}$ femora have increased trabecular number. Goldner's trichrome stain of femora from 8-mo-old *C/EBPα*$^{+/-}$ or *C/EBPα*$^{+/+}$ mice.

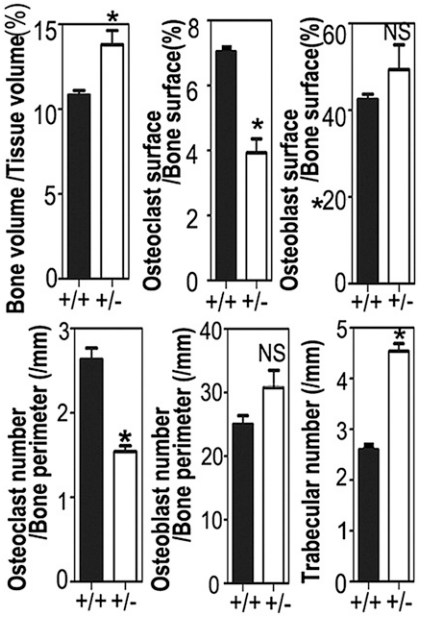

Fig. S5. Histomorphometric analysis of femora from 8-mo-old *C/EBPα*$^{+/+}$ and heterozygous *C/EBPα*$^{+/-}$ mice. Histomorphometric analysis indicates that *C/EBPα*$^{+/-}$ femora have an increase in bone volume/tissue volume and trabecular number and a decrease in osteoclast surface/bone surface and osteoclast number/bone perimeter. *$P < 0.05$. NS, not significant.

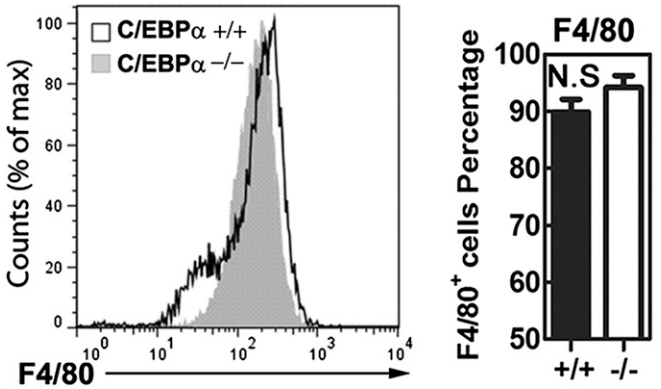

Fig. S6. Flow cytometry analyses with a mature macrophage marker F4/80. Embryonic day 17.5–18 livers were used as a source of myeloid cells, which were then stimulated with M-CSF alone for macrophage differentiation analysis. No significant difference in the percentage of F4/80^{+} cells was observed between the *C/EBPα*$^{+/+}$ and *C/EBPα*$^{-/-}$ groups. max, maximum; N.S, not significant.

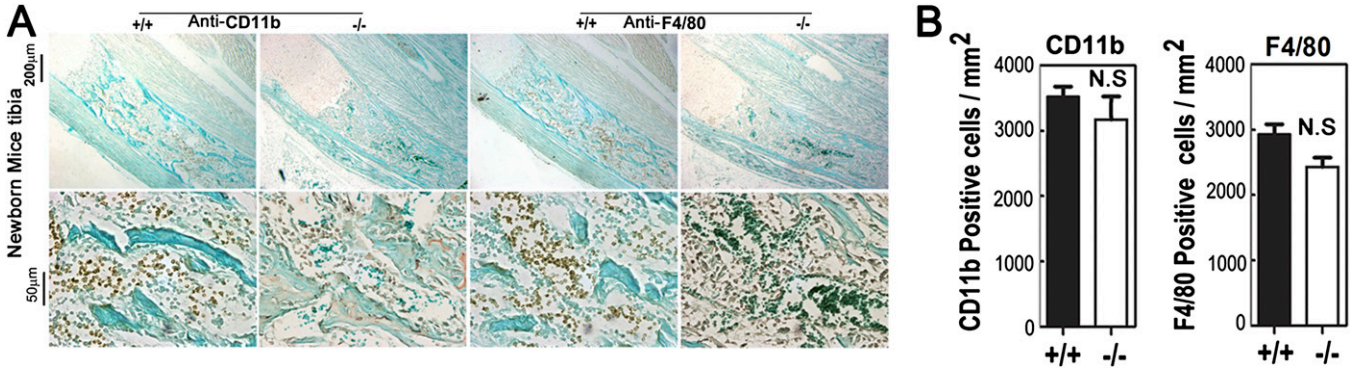

Fig. S7. Immunostaining for monocyte markers (CD11b and F4/80). (*A*) Immunostaining for a monocyte marker [integrin αM (CD11b)] and the mature macrophage marker F4/80 in C/*EBPα*$^{+/+}$ and C/*EBPα*$^{-/-}$ tibiae. (*B*) Quantification of CD11b^{+} and F4/80^{+} cells. There was no significant difference in the number of CD11b^{+} or F4/80^{+} cells in C/*EBPα*$^{-/-}$ tibiae compared with the C/*EBPα*$^{+/+}$ control.

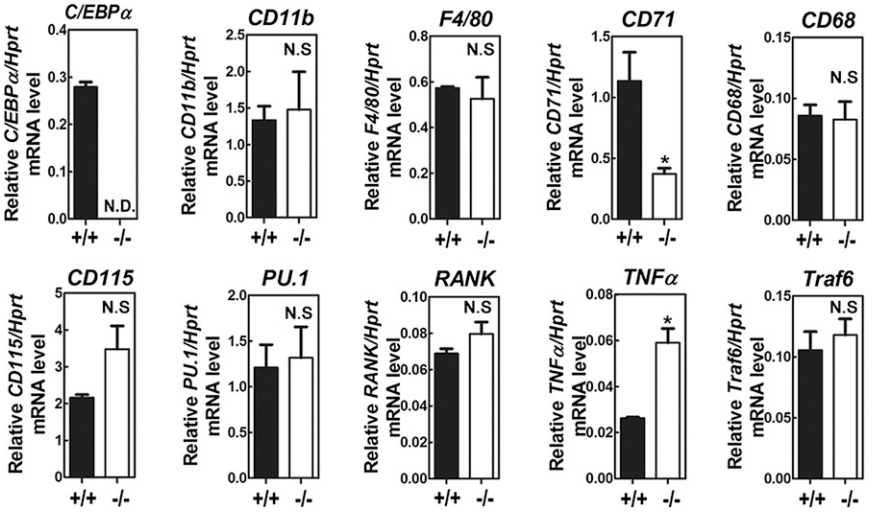

Fig. S8. qPCR analysis of genes important for macrophage differentiation in C/*EBPα*$^{+/+}$ and C/*EBPα*$^{-/-}$ MBM-derived monocyte/macrophage-like cells. RT-qPCR was used to examine the expression of genes important for macrophage differentiation in C/*EBPα*$^{+/+}$ and C/*EBPα*$^{-/-}$ MBM cells cultured with M-CSF alone to generate monocyte/macrophage-like cells. Consistent with our findings in M-CSF cultured MBM cells and mouse tibiae, there was no significant change in the expression of F4/80 between C/*EBPα*$^{+/+}$ and C/*EBPα*$^{-/-}$ MBM-derived monocyte/macrophage-like cells. In addition, there was no significant difference in the expression of genes common to macrophages and OCs (e.g., *PU.1*, *RANK*, *Traf6*, *CD11b*, *CD115*, *CD68*]. Interestingly, C/*EBPα*$^{-/-}$ MBM-derived monocyte/macrophage-like cells did have a significant decrease in the expression of *transferring receptor* (*CD71*) and a significant increase in the expression of the mature macrophage-related gene *TNFα*. The loss of C/*EBPα* expression was confirmed, because C/*EBPα* expression was not detected (N.D.) in C/*EBPα*$^{-/-}$ MBM-derived monocyte/macrophage-like cells. *$P < 0.05$.

Table S1. Primers and Taqman probes used for qPCR

Gene symbol	Applied Biosystems Taqman assay ID	Primers used for semi-qPCR	
		Forward primers (5′-3′)	Reverse primers (5′-3′)
Acp5	Mm00475698_m1	CAGCAGCCCAAAATGCCT	TTTTGAGCCAGGACAGCTGA
Calcr	Mm00432271_m1		
Car2	Mm00501572_m1		
Cd68	Mm03047340_m1		
Cebpa (C/EBPα)	Mm00514283_s1		
Cebpb (C/EBPβ)	Mm00843434_s1		
Csf1r (CD115)	Mm01266652_m1		
Ctsk	Mm00484039_m1	GGGCTCAAGGTTCTGCTGC	TGGGTGTCCAGCATTTCCTC
Emr1 (F4/80)	Mm00802529_m1		
Fos (c-Fos)	Mm00487425_m1	CGGGTTTCAACGCCGACTA	TTGGCACTAGAGACGGACAGA
Hprt	Mm01545399_m1	GGTGGAGATGATCTCTCAACTTTAA	AGGAAAGCAAAGTCTGCATTGTT
Itgam (CD11b)	Mm00434455_m1		
Itgb3	Mm00443980_m1		
Mmp14	Mm00485054_m1		
Mmp9	Mm00442991_m1		
Mst1r	Mm00436365_m1		
Myo1D	Mm01296373_m1		
Nfatc1	Mm00479445_m1	TGCCTTTTGCGAGCAGTATCT	CAGGCAAGGATGGGCTCATAT
Oscar	Mm00558665_m1		
Pparg	Mm01184322_m1		
Rcan2	Mm00472671_m1		
Runx2	Mm00501584_m1		
Sfpi1 (PU.1)	Mm00488142_m1		
Tfrc (CD71)	Mm00441941_m1		
Tnf (TNF-α)	Mm00443260_g1		
Tnfrsf11a (Rank)	Mm00437135_m1		
Traf6	Mm00493836_m1		

The right column lists the probes for qRT-PCR while the left column lists the primer for semi-qPCR. The definitions for the gene symbols are as follows: *Acp5*: *acid phosphatase 5, tartrate resistant*; *Calcr*: *calcitonin receptor*; *Car2*: *carbonic anhydrase 2*; *Cd68*: *CD68 antigen*; *Cebpa*: *CCAAT/enhancer binding protein (C/EBP), alpha*; *Cebpb*: *CCAAT/enhancer binding protein (C/EBP), beta*; *Csf1r (CD115)*: *colony stimulating factor 1 receptor*; *Ctsk*: *cathepsin K*; *Emr1 (F4/80)*: *EGF-like module containing, mucin-like, hormone receptor-like sequence 1*; *Fos (c-Fos)*: *FBJ osteosarcoma oncogene*; *Hprt*: *hypoxanthine guanine phosphoribosyl transferase*; *Itgam (CD11b)*: *integrin alpha M*; *Itgb3*: *integrin beta 3*; *MMP14*: *matrix metallopeptidase 14*; *Mmp9*: *matrix metallopeptidase 9*; *Mst1r*: *macrophage stimulating 1 receptor (c-met-related tyrosine kinase)*; *Myo1D*: *myosin ID*; *Nfatc1*: *nuclear factor of activated T-cells, cytoplasmic, calcineurin-dependent 1*; *Oscar*: *osteoclast associated receptor*; *Pparg*: *peroxisome proliferator activated receptor gamma*; *Rcan2*: *regulator of calcineurin 2*; *Runx2: runt related transcription factor 2*; *Sfpi1 (PU.1)*: SFFV *proviral integration 1*; *Tfrc (CD71)*: *transferrin receptor*; *TNFalpha*: *tumor necrosis factor*; *Tnfrsf11a*: *tumor necrosis factor receptor superfamily, member 11a*; *Traf6*: *TNF receptor-associated factor 6*.